Supporting Information

Application of $W_{1.33}CT_z$ MXene obtained by hydrothermal etching as an additive to enhance the electrochemical energy storage properties of binder-free $Ti_3C_2T_x$ MXene films

Alexey Tsyganov,*[a] Maria Vikulova,[a] Ilya Zotov,[a] Evgeniy Korotaev,[b] Ilya Plugin,[a] Victor Sysoev,[a] Demid Kirilenko,[c] Maxim Rabchinskii,[c] Artur Asoyan,[d] Alexander Gorokhovsky[a] and Nikolay Gorshkov*[a]

[a] Yuri Gagarin State Technical University of Saratov, 77 Polytecnicheskaya Street, 410054 Saratov, Russia.

[b] Nikolaev Institute of Inorganic Chemistry, Siberian Branch, Russian Academy of Sciences, 630090 Novosibirsk, Russia

[c] Ioffe Institute, 26 Politekhnicheskaya Street, 194021 Saint Petersburg, Russia

[d] Peoples Friendship University of Russia, 6 Miklukho-Maklaya Street, Moscow, 117198, Russia

***Corresponding author:**

Alexey Tsyganov: tsyganov.a.93@mail.ru

Nikolay Gorshkov: gorshkov.sstu@gmail.com

Synthesis of $Ti_3C_2T_x$

The MAX phase Ti_3AlC_2 powder was obtained by the molten salt method. Aluminium (99% Xinchang Tuan Machinery Co., Ltd.), titanium (99% Himkraft LLC) and titanium carbide (99% Himkraft LLC) powders were used. The starting powders were taken in the molar ratio Ti:Al:TiC as 1:1.4:2. The mixture was homogenized in a monoplanetary mill using grinding media in the form of ZrO_2 balls. The resulting batch was then pressed into cylindrical bodies with a diameter of 12 mm and a height of 20 mm by uniaxial pressing at a pressure of 10 MPa. In order to prevent oxygen access in the early stages of heating, the produced cylindrical granules were placed in a eutectic NaCl-KCl melt preheated to 800 °C. The crucible was covered with a lid to prevent evaporation of the melt and placed in a muffle furnace at 1250 °C for 3 hours in an air environment. At the end of the reaction, the crucible was cooled to room temperature. The resulting product was washed with deionized water and HCl solution (6 M). As a result of the processes, the Ti_3AlC_2 MAX phase powder was obtained.

Further processing of Ti_3AlC_2 MAX phase powder by hydrothermal etching allowed us to obtain multilayer $Ti_3C_2T_x$ MXene powder. Lithium fluoride and hydrochloric acid (HCl) were used. 2.25 g of Ti_3AlC_2 MAX phase powder and 60 ml of 6 M hydrochloric acid were placed in a 150 ml Teflon cup. The Teflon cup was then placed in a steel bowl and sealed. The autoclave was maintained at 140 °C for 20 hours. After natural cooling, the resulting mixture was removed and washed with deionised water. The wet $Ti_3C_2T_x$ MXene powder was further used. The preparation of single $Ti_3C_2T_x$ MXene nanosheets was carried out by intercalation of the interlayer space with TMAOH molecules ($C_4H_{13}NO$, 5% aqueous solution). 5 ml of TMAOH solution (5 wt%) was added to 1 g of $Ti_3C_2T_x$ MXene. The intercalation process was carried out for 1 h under vigorous stirring. The intercalated $Ti_3C_2T_x$ MXenes were then washed several times with deionized water to maximize powder purification. The resulting precipitate was then subjected to ultrasonic treatment until a homogeneous colloidal solution of single flake $Ti_3C_2T_x$ was obtained.

Material characterization

In Figure S1, the intense diffraction peaks of Ti_3AlC_2 MAX (JCPDF 52-0857) are clearly visible, indicating that the MAX phase powder was successfully synthesized. The hydrothermal treatment of Ti_3AlC_2 in a mixture of LiF and HCL 6M allowed us to obtain multilayer $Ti_3C_2T_x$, as evidenced by the disappearance of the main diffraction peaks and the appearance of a diffraction peak at $2\theta \approx 6°$, corresponding to the crystallographic plane (002).

The obtained Ti_3AlC_2 MAX phase powder (Figure S2a) showed the typical layered morphology of MAX phases. After treatment in LiF/HCl mixture, the formation of accordion-like particles typical of multilayered MXenes was observed (Figure S2b). Figure S2c shows the TEM image of the $Ti_3C_2T_x$ nanosheet, confirming the successful delamination of the MXene. The cross-sectional SEM image (Figure S2d) of binder-free $Ti_3C_2T_x$ films shows the repeated stacking of nanosheets in horizontal orientation. Similar films have been used as supercapacitor electrodes.

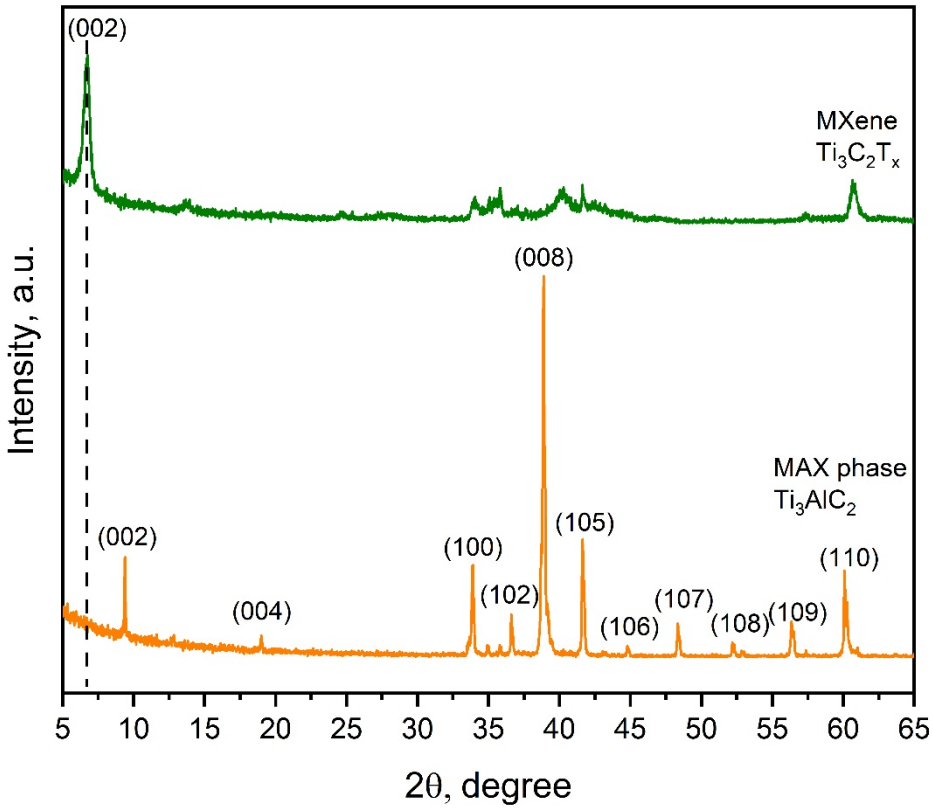

Figure S1. XRD pattern of the obtained powders Ti_3AlC_2 MAX phase and $Ti_3C_2T_x$ MXene

Figure S3 shows the high-resolution XPS spectrum of the $Ti_3C_2T_x$ film in the Ti 2p, C 1s, O 1s, Cl 2p and F 1s regions. The results of the peak fitting are given in the table S2. A summary of global atomic percentages (at.%) of $Ti_3C_2T_x$ sample obtained from their XPS survey spectra is presented in table S1. Based on the results of the XPS spectrum fitting (table S1-S2), the chemical formula was determined to be $Ti_{2.97}C_2O_{0.77}(OH)_{0.72}Cl_{0.73}F_{0.39}\cdot 0.27H_2O$.

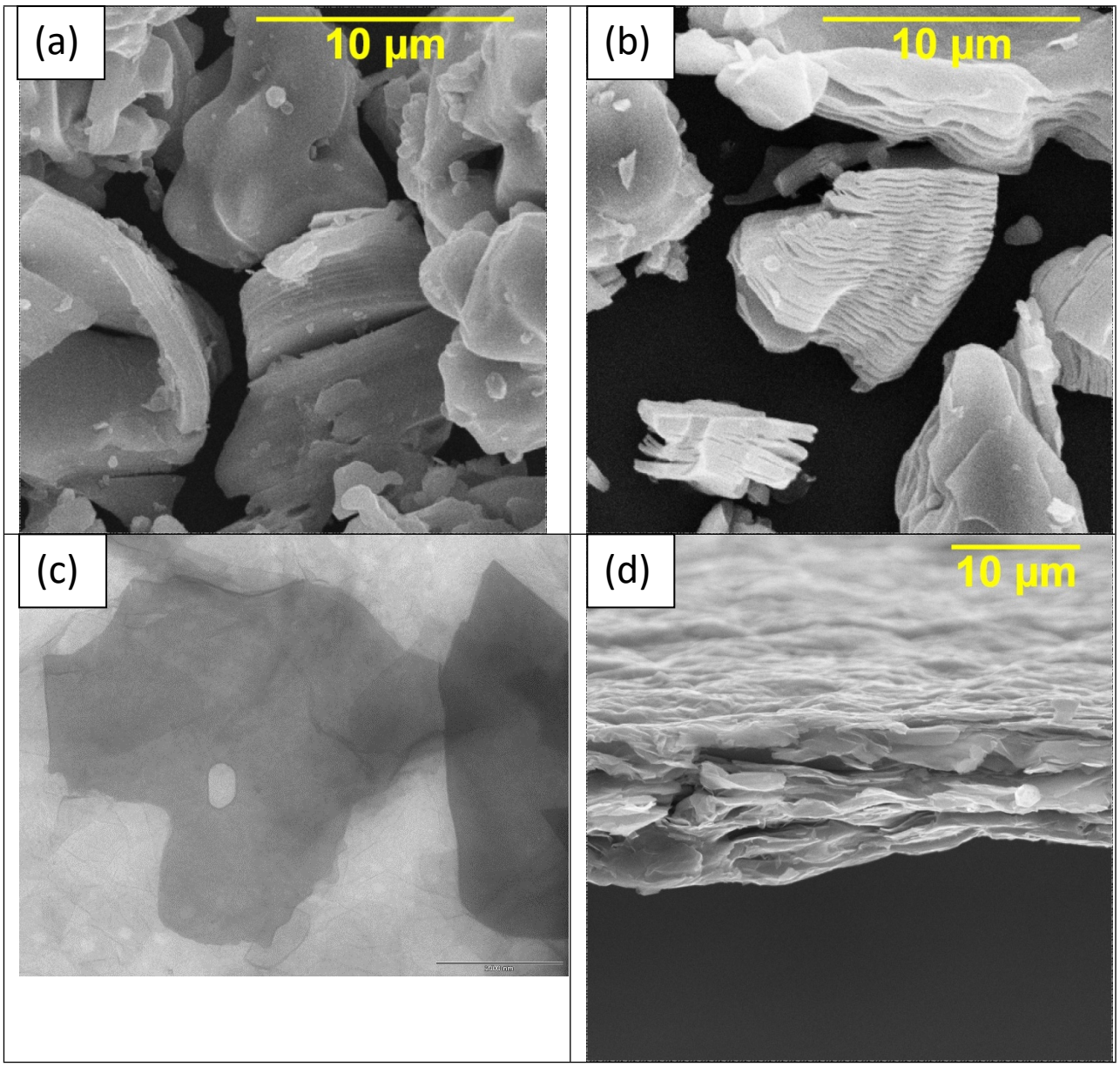

Figure S2. SEM images of **(a)** Ti_3AlC_2 and **(b)** $Ti_3C_2T_x$ MXene. **(c)** TEM image of $Ti_3C_2T_x$ MXene nanosheet. **(d)** SEM image of cross section of binder-free film of delaminated MXene.

Table S1 Summary of global atomic percentages (at.%) of $Ti_3C_2T_x$ sample obtained from their XPS survey spectra.

MXene film	Ti, at.%	C, at.%	O, at.%	Cl, at.%	F, at.%	N, at.%
$Ti_3C_2T_x$	20.2	52.0	20.5	4.0	2.3	1

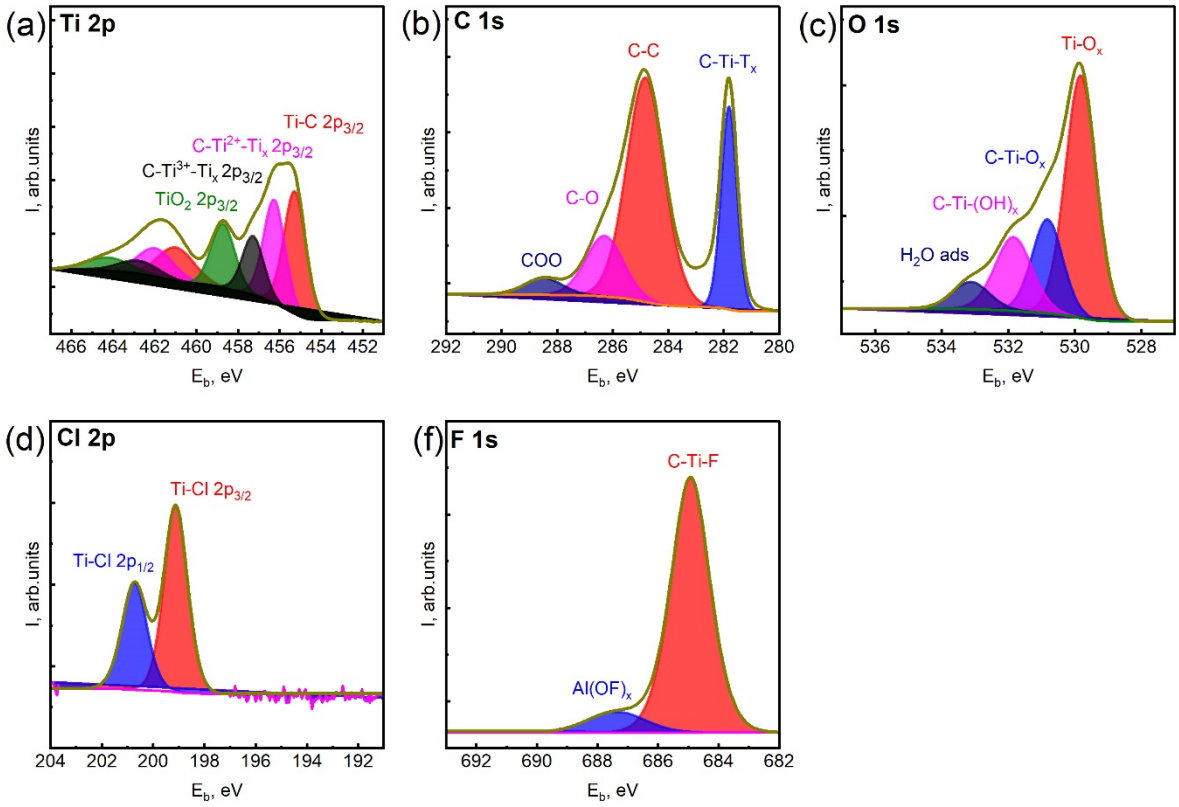

Figure S3. High-resolution XPS spectra of $Ti_3C_2T_x$ MXene in the **(a)** Ti 2p region, **(b)** C 1s region, **(c)** O 1s region, **(d)** Cl 2p region and **(e)** F 1s region.

Table S2. XPS peak fitting results for $Ti_3C_2T_x$ MXene.

Region	BE[eV][a]	FWHM[eV]	Fraction	Assigned to
Ti $2p_{3/2}(2p_{1/2})$	455.3 (461.0)	1.3(2.1)	0.34	Ti-C
	456.3 (462.1)	1.3(2.0)	0.29	C-Ti^{2+}-T_x
	457.3 (462.9)	1.3(1.8)	0.17	C-Ti^{3+}-T_x
	458.8 (464.4)	(2.1)	0.20	TiO_2
C 1s	281.8	0.8	0.21	C-Ti-T_x
	284.8	1.7	0.56	C-C
	286.3	1.6	0.18	C-O
	288.5	1.6	0.05	COO
O 1s	529.9	1.2	0.53	Ti-O_x
	530.9	1.2	0.20	C-Ti-O_x
	531.9	1.4	0.19	C-Ti-$(OH)_x$

	533.2	1.2	0.07	C-Mo-H_2O_{ads}
F 1s	684.9	1.7	0.93	C-Ti-F
	687.4	2	0.07	$Al(OF)_x$
Cl $2p_{3/2}(2p_{1/2})$	199.1(200.8)	1.4(1.4)	1	Ti-Cl

Table S3 Summary of global atomic percentages (at.%) of $W_{1.33}CT_z$ sample obtained from their XPS survey spectra.

MXene film	**W, at.%**	**C, at.%**	**O, at.%**	**Cl, at.%**	**F, at.%**	**Y, at.%**
$W_{1.33}CT_z$	14.1	44.0	39.5	1.7	0.3	0.5

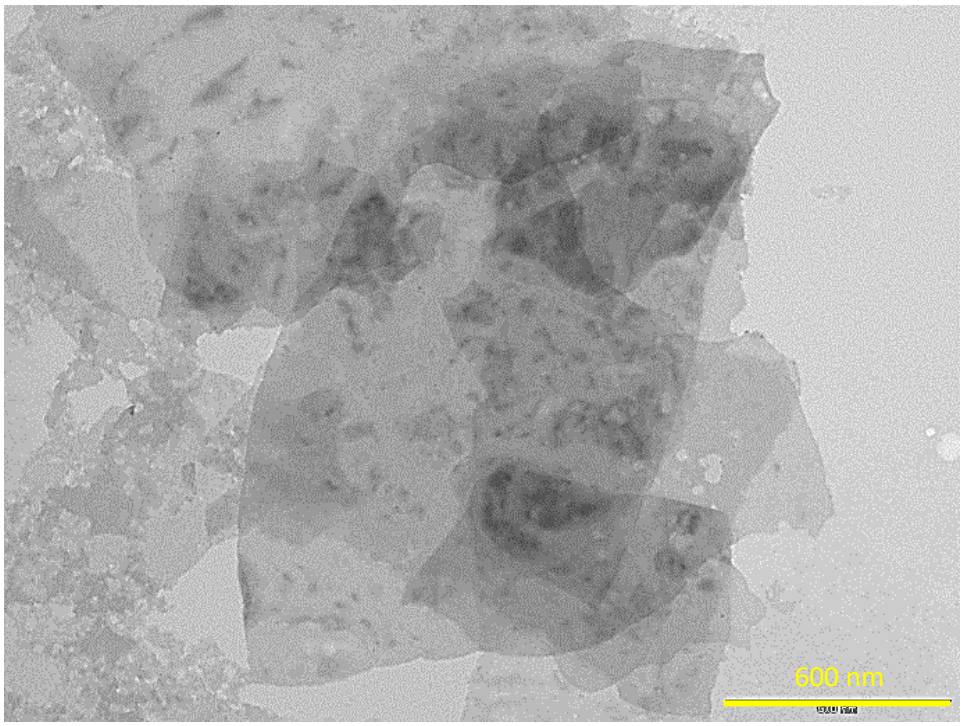

Figure S4. TEM image of $W_{1.33}CT_z$ MXene nanosheet.

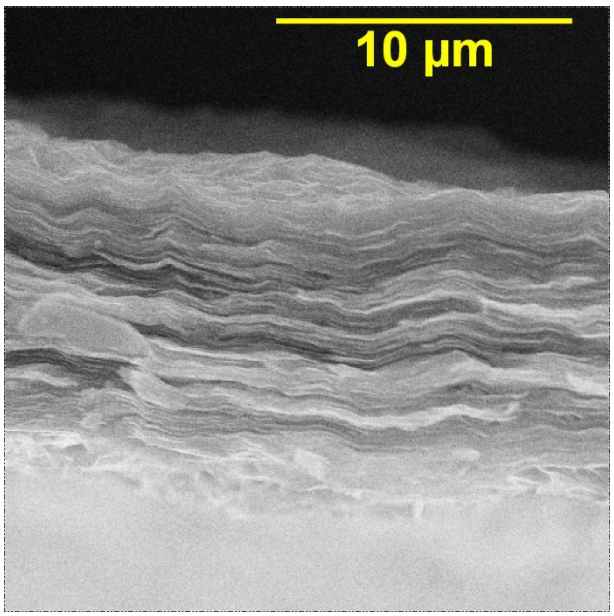

Figure S5. SEM image of cross section of Ti3C2Tx/W1.33CTz(40wt.%) binder-free film of delaminated MXene.

Table S4. XPS peak fitting results for $W_{1.33}CT_z$ MXene.

Region	BE[eV][a]	FWHM[eV]	Fraction	Assigned to
W 4f7/2(4f5/2)	32.4 (34.5)	0.8(0.8)	0.38	W-C
	33.2 (35.3)	0.9(1.0)	0.10	W-T_z
	35.2 (37.3)	1.3(1.4)	0.52	WO3
C 1s	282.4	1.1	0.13	C-W-T_z
	284.8	2.6	0.68	C-C
	286.3	1.6	0.13	C-O
	288.4	1.6	0.07	COO
O 1s	530.2	1.4	0.64	W-O_x
	531.2	1.4	0.22	C-W-O_x
	532.2	1.3	0.10	C-W-$(OH)_x$
	533.3	1.3	0.04	C-W-H_2O_{ads}
F 1s	684.8	2.5	0.51	C-W-F
	688.8	2.5	0.49	Al$(OF)_x$
Cl $2p_{3/2}(2p_{1/2})$	198.5(200.8)	1.3(1.3)	1	W-Cl

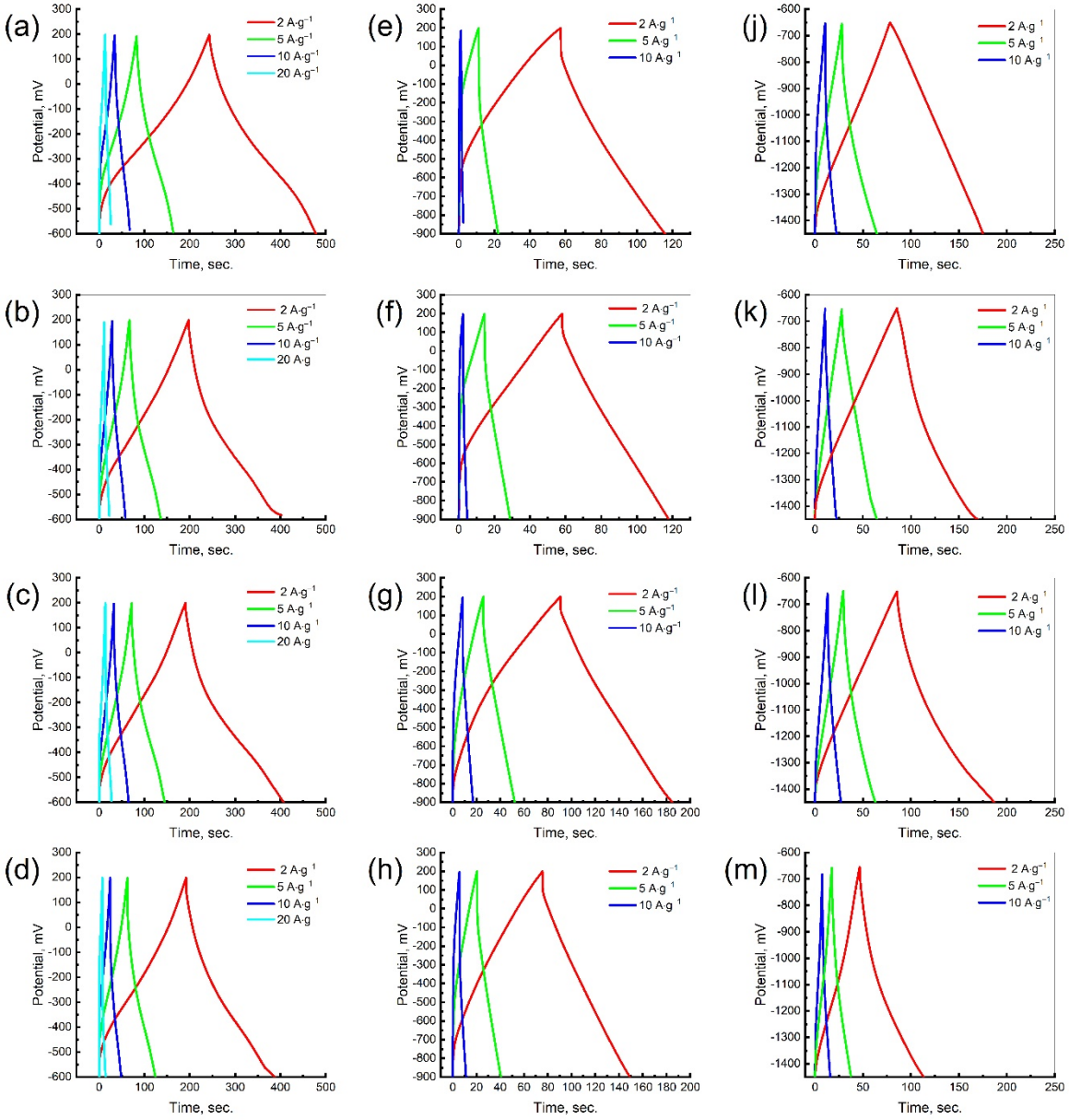

Figure S6. GCD curves of $Ti_3C_2T_x/W_{1.33}CT_z$ MXene films at different current densities. (**a**) TW0 in H_2SO_4, (**b**) TW10 in H_2SO_4, (**c**) TW20 in H_2SO_4, (**d**) TW40 in H_2SO_4, (**e**) TW0 in LiCl, (**f**) TW10 in LiCl, (**g**) TW20 in LiCl, (**h**) TW40 in LiCl, (**j**) TW0 in KOH, (**k**) TW10 in KOH, (**l**) TW20 in KOH, (**m**) TW40 in KOH.

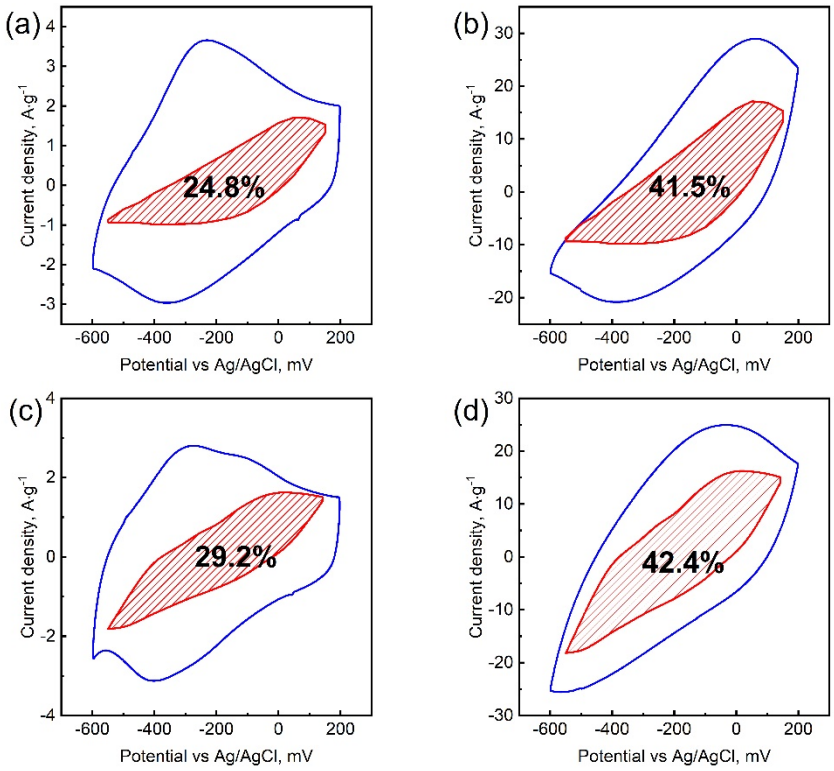

Figure S7. Contribution of surface capacitive processes to charge accumulation in H2SO4 electrolyte for $Ti_3C_2T_x$ at 5mV·s^{-1} (**a**), $Ti_3C_2T_x$ at 50mV·s^{-1} (**b**), $Ti_3C_2T_x/W_{1.33}CT_z$(20wt.%) at 5mV·s^{-1} (**c**) and $Ti_3C_2T_x/W_{1.33}CT_z$(20wt.%) at 50mV·s^{-1} (**d**).

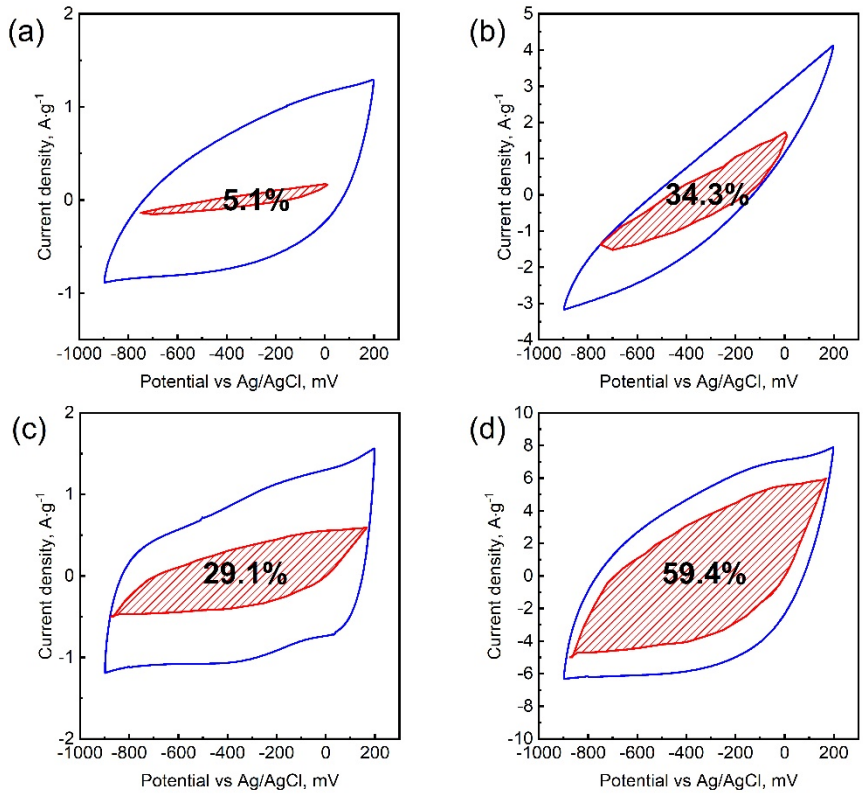

Figure S8. Contribution of surface capacitive processes to charge accumulation in LiCl electrolyte for $Ti_3C_2T_x$ at 5mV·s^{-1} (**a**), $Ti_3C_2T_x$ at 50mV·s^{-1} (**b**), $Ti_3C_2T_x/W_{1.33}CT_z$(20wt.%) at 5mV·s^{-1} (**c**) and $Ti_3C_2T_x/W_{1.33}CT_z$(20wt.%) at 50mV·s^{-1} (**d**).

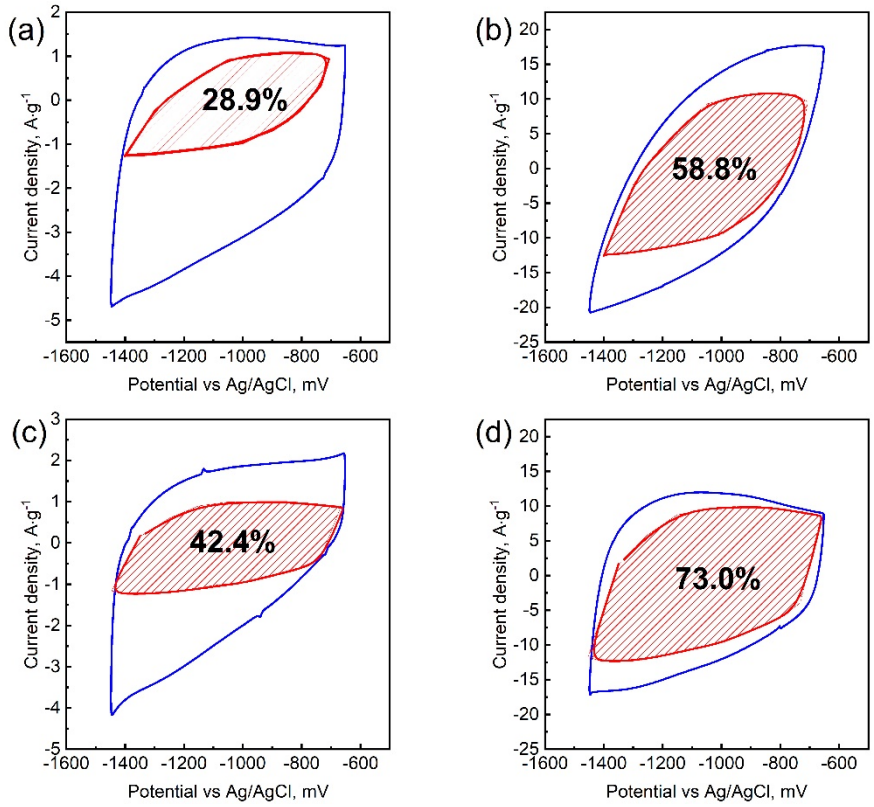

Figure S9. Contribution of surface capacitive processes to charge accumulation in KOH electrolyte for $Ti_3C_2T_x$ at 5mV·s^{-1} (**a**), $Ti_3C_2T_x$ at 50mV·s^{-1} (**b**), $Ti_3C_2T_x/W_{1.33}CT_z$(20wt.%) at 5mV·s^{-1} (**c**) and $Ti_3C_2T_x/W_{1.33}CT_z$(20wt.%) at 50mV·s^{-1} (**d**).

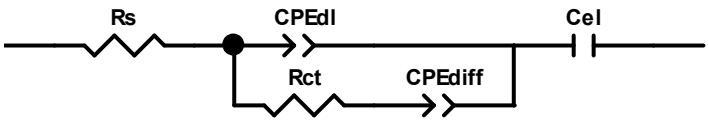

Figure S10. Equivalent circuit of impedance.

Table S5. Impedance parameters of $Ti_3C_2T_x/W_{1.33}CT_z$ MXene electrodes in H_2SO_4, LiCl and KOH electrolytes.

Electrolyte Concentration	H_2SO_4				LiCl				KOH		
MXene film	W0-T100	W10-T90	W20-T80	W40-T60	W0-T100	W10-T90	W20-T80	W40-T60	W0-T100	W20-T80	W40-T60
R_s, Ohm	4.081	4.14	4.021	4.327	8.818	9.213	8.82	8.514	1.867	2.681	2.686
Q_{dl}, $F·s^{(a-1)}$	7.88E-05	3.65E-05	2.03E-03	2.05E-03	0.021	0.123	0.494	0.635	0.065	8.01E-04	0.015
a_{dl}	1	0.999	0.65	0.631	0.506	0.736	0.4	0.721	0.154	0.666	4.40E-01
Q_{diff}, $F·s^{(a-1)}$	0.281	0.613	0.565	0.378	0.025	0.052	0.13	0.136	0.049	0.148	3.841
a_{diff}	0.39	0.237	0.341	0.445	0.289	0.374	0.513	0.385	0.65	0.178	0.125
R_{ct}, Ohm	0.507	0.106	1.019	1.121	1.515	1.654	2.375	1.638	2.273	0.495	0.762
C_{el}, F	-	0.45	0.342	-	-	-	-	-	-	0.327	0.846